Supplementary Material

Theoretical estimates of exposure timescales of protein binding sites on DNA regulated by nucleosome kinetics

Jyotsana J. Parmar[1], Dibyendu Das[2] and Ranjith Padinhateeri[1]

[1]Department of Biosciences and Bioengineering, Indian Institute of Technology Bombay, Mumbai 400076, India and [2]Department of Physics, Indian Institute of Technology Bombay, Mumbai 400076, India

1 Competition between a DNA-binding protein and a nucleosome: importance of exposure time

What effect does nucleosome kinetics have on DNA exposure, and as a result on protein binding? We consider a simple model in which there is a single protein binding site. The site may be exposed or covered by a nucleosome stochastically, with a binding rate k_+ and unbinding rate k_-. Apart from that, a transcription factor (TF) may also bind with rate r_p if the site is exposed (not covered by nucleosome). Here the TF competes with the nucleosome to gain access and thereby bind to the site, see Figure S1A. Note that for this problem, the ratio of k_+/k_- gives the nucleosome occupancy. That is, the average nucleosome density $\rho = k_+/(k_+ + k_-)$. An interesting question is, how long one has to wait for the protein to bind to the site for the first time (first passage time), if we make nucleosome kinetics slow or fast, maintaining a fixed density. In other words, if we fix the ratio of k_+/k_- and vary k_+ and k_- individually, will the first passage time (FPT) distributions of TF binding get affected? If it does, it would show that TF binding history does get affected by nucleosome kinetics and cannot be predicted from nucleosome occupancy alone.

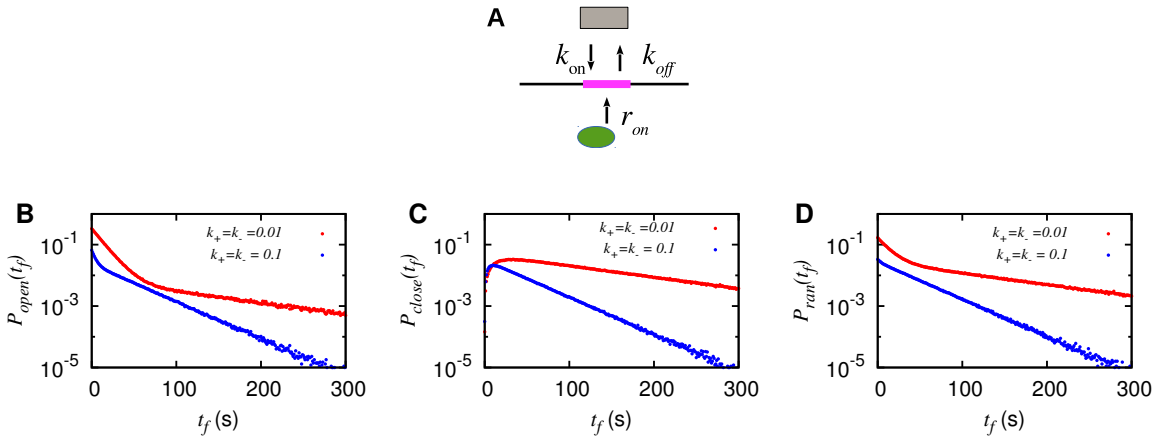

Figure S1: (A) Schematic showing a single binding site (pink patch), where nucleosome (gray block) and TF (green oval) are competing to bind with their respective rates as shown. (B) FPT distributions of TF binding with the site open at $t = 0$. Red: $k_+ = k_- = 0.01s^{-1}$ with $T_f^{\text{open}} = 29.4s$ and SD $= 61.9s$, blue: $k_+ = k_- = 0.1s^{-1}$ with $T_f^{\text{open}} = 29.4s$ and SD $= 34.5s$. (C) Simulation starts from a closed site; red: $k_+ = k_- = 0.01s^{-1}$ with $T_f^{\text{close}} = 128.8s$ and SD $= 116.5s$, blue: $k_+ = k_- = 0.1s^{-1}$ with $T_f^{\text{close}} = 39.7s$ and SD $= 35.6s$. (D) Simulation starts from a randomly chosen open or closed site with equal probability. Red: $k_+ = k_- = 0.01s^{-1}$ with $T_f = 78.4s$ and SD $= 106.8s$, blue: $k_+ = k_- = 0.1s^{-1}$ with $T_f = 34.6s$ and SD $= 35.5s$. TF binding rate in all the cases is $r_p = 0.06s^{-1}$.

Let t_f be the FPT for TF to bind at the site. In Figure S1(B)-(D), we present distributions of t_f obtained under different initial conditions, using numerical simulations. In each figure, we consider two cases (i) $k_+ = k_- = 1/10s^{-1}$ (blue curves) and (ii) $k_+ = k_- = 1/100s^{-1}$ (red curves) such that the occupancy $= k_+/(k_+ + k_-) = 0.5$ in both the cases. The TF binding rate $r_p = 1/15s^{-1}$, for both (i) and (ii). The probability distributions appearing in the Figures S1(B)-(D) are defined below.

If at time $t = 0$ the site is exposed (open), let the probability distribution of t_f be $P_{\rm open}(t_f)$ (see Figure S1(B)) and the mean be $T_f^{\rm open}$. For this initial condition, $T_f^{\rm open}$ for both (i)(blue) and (ii)(red) are the same, however the distributions and hence the standard deviations (SD) are very different (see figure caption). Similarly, if at $t = 0$ the site is covered by nucleosome (closed), let the probability distribution of t_f be denoted by $P_{\rm close}(t_f)$, and mean by $T_f^{\rm close}$. In this situation, the distributions (see Figure S1(C)) are different implying that the SDs are different. Moreover, in this case, the means $T_f^{\rm close}$ are also different. Finally, if we start from a randomly open or closed state with equal probability, let the FPT distribution be called $P_{\rm ran}(t_f)$, and mean be T_f. We find that the distribution, SD, and mean are all different (see Figure S1(D)). For this simple model, the mean FPT values can be analytically derived as shown below.

1.1 Formulas for the "mean" first passage times

Starting from the open state, two events are possible – either binding of a TF or binding of a nucleosome. Once a TF binds, the first passage happens, while if a nucleosome binds, the first passage is delayed by additional mean time $T_f^{\rm close}$. Thus we have,

$$T_f^{\rm open} = \frac{1}{(k_+ + r_p)} + \frac{k_+}{(k_+ + r_p)} T_f^{\rm close} \tag{S1}$$

Similarly, starting from the closed state, the only possible event is nucleosome unbinding, and there is a subsequent delay of mean time $T_f^{\rm open}$. Thus,

$$T_f^{\rm close} = \frac{1}{k_-} + T_f^{\rm open} \tag{S2}$$

Solving the above,

$$T_f^{\rm open} = \frac{1}{r_p}\left(1 + \frac{k_+}{k_-}\right) \tag{S3}$$

$$T_f^{\rm close} = \frac{1}{k_-} + \frac{1}{r_p}\left(1 + \frac{k_+}{k_-}\right) \tag{S4}$$

In case at $t = 0$, the site may be either open or closed by the nucleosome, the mean first passage time T_f would be an weighted average of $T_f^{\rm open}$ and $T_f^{\rm close}$, i.e.

$$T_f = \frac{k_- T_f^{\rm open} + k_+ T_f^{\rm close}}{k_+ + k_-} \tag{S5}$$

Although from Eq. S3, we see that $T_f^{\rm open}$ depends only on the ratio k_+/k_- i.e., it is predictable from nucleosome occupancy, the same is not the case for $T_f^{\rm close}$ or T_f. Moreover, when we numerically studied (see above) the full probability distributions $P_{\rm open}(t_f)$, $P_{\rm close}(t_f)$, and $P_{\rm ran}(t_f)$, we found that those depend on individual values of k_+ and k_- and not merely on the ratio k_+/k_-. Thus, the protein binding histories will be distinct for different nucleosome kinetics. In particular, the SDs, shown in the caption of Figure S1, of the TF binding timescales is much higher for the red curves than for the blue curves. This would produce comparatively higher noise in protein binding (and consequently further regulatory activities that it triggers) in one case compared to the other.

2 Gap distribution $P_{\rm in}(l)$ and its effect on $T_{\rm av}$

If the distribution of the initial nucleosome location (l) from the barrier is chosen in steady state, then $P_{\rm in} = P_{\rm ss}$, where $P_{\rm ss}(l) = (1-\xi)\xi^l$ for $l \geq 0$ and $P_{\rm ss} = 0$ for $l < 0$. The constant ξ depends on the ratio of dissociation rate to binding rate and is given by the relationship $\frac{k_{\rm off}}{k_{\rm on}} = \frac{\xi^k}{1-\xi}$, as shown by Krapivsky et al. in ref. [1]. Smaller is the ratio of the rates, smaller is the typical gap length scale $l_{\rm ss} = -1/\ln\xi$ and larger is the density of nucleosomes. In the main manuscript, we have used a distribution $P_{\rm ss}(l - l_{\rm min})$ with shifted argument; this is due to the fact that at $t = 0$, next to the barrier, a stretch of length $l_{\rm min}$ is unoccupied by nucleosomes. As per our above definition, the profile of such a function is shown in Figure S2. Note that $T_{\rm av}$ is obtained using $P_{\rm ss}(l - l_{\rm min})$ in Eq. **2** of the main manuscript.

Also, note that $P_{\rm in}$ depends on the initial experimental design, and that in turn determines $T_{\rm av}$. As an alternative to steady state distribution, an experimentalist may control initial separations $l \in [l_{\rm min}, L]$ to be equally likely up to a maximum $l = L$, then $P_{\rm in} = 1/(L - l_{\rm min})$ and hence $T_{\rm av} = \sum_{l=l_{\rm min}}^{L} T_l/(L - l_{\rm min})$.

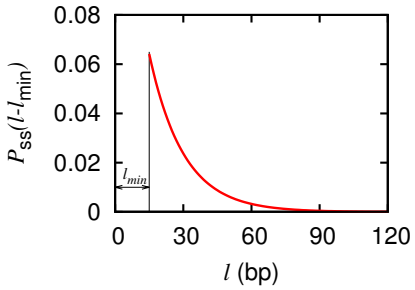

Figure S2: The l dependence of the distribution $P_{\rm ss}(l - l_{\rm min})$.

3 T_l Vs l – physical explanation

In Figure 3(A) of the manuscript, we have shown the T_l versus l curve for uniform sequence ($k_{\rm off}$ = constant). Here we provide some more explanation for the BL shape of the curve arising out of the Eqs. **3-6** appearing in the main manuscript.

For $l_{\rm min} \leq l < k$ (Case 1), the timescales T_l have a steady rise with l but just before going over to the branch in Case 2, has a slight dip in value after passing through a maximum (see Figure 3(A), main manuscript). The steady rise may be attributed to the rise in average delay due to increase in possible events that misses binding to the m-patch, just after nucleosome I (in Figure 2(A)) dissociates. But when l gets close to k, and the new gap length $\tilde{l} \approx l+k+l_{\rm ss} \approx 2k$, where $l_{\rm ss} = -1/\ln\xi$ (see above section) is the typical gap length, then two side-by-side bindings of nucleosome may happen after the nucleosome I dissociation. The latter events would cover the m-patch directly, bringing down the average delay. Thus over the range $l \in (k - l_{\rm ss}, k)$ one expects the T_l to diminish. By varying $l_{\rm ss}$, we have checked using our theoretical formula that the peak position is indeed near $k - l_{\rm ss}$ as expected from the above reasoning.

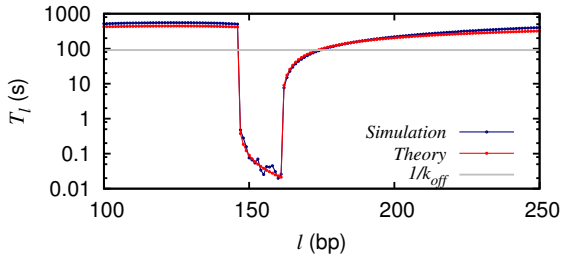

Figure S3: Figure 3(A) in the main manuscript is reproduced here as a log-linear plot to show the nature of middle region of the BL curve clearly.

In the regime $k \leq l < (l_1 + m + k)$ (Case 2 of main manuscript), from Figure 3(A), the l dependence of T_l is not evident. The values of T_l are not zero but of the order of $\sim 1/[k_{\rm on}(l - k + 1)]$ – hence T_l should decrease with l. This behavior is clearly seen when T_l versus l is plotted on a log-linear scale – see Figure S3.

In Eq. **5** for Case 3, the average delay after direct binding events (with probability $k_{\rm on}/\lambda_l$) missing the m-patch has been written as $1/2k_{\rm off} + T_l/2 + T_{l'}/2$ within an approximation. The rational is as follows. After the binding of a nucleosome between nucleosome I and the barrier, a gap of length $l^{'}$ is created. Now subsequently, we assume that two mutually exclusive events may happen. Either the newly bound nucleosome dissociate with probability 1/2 and contribute a further delay of average time T_l, or if nucleosome I dissociate with probability 1/2, the delay is $T_{l'}$. The average waiting time for neither of these two events to happen is $1/2k_{\rm off}$. There are other ways in which this delay could have been approximated, e.g. as $T_{l'}$. But due to the presence of nucleosome I at l, the gap distribution is so strongly conditioned away from steady state, that the actual delays are far from $T_{l'}$. We verified that the approximation used in the paper does better than the latter one.

In Eq. **6** for case 4, because of the huge gap l, binding events are principal determinants of the

kinetics. If the patch gets directly covered, the contribution to T_l is only $1/\lambda_l$. But quite often the newly bound nucleosome misses the m-patch introducing larger delays in coverage like the above cases. What is distinct compared to all the other cases, is the possibility of two nucleosomes binding in the gap between $m + l_1$ and l. The possibility of a second binding arises in multiple ways as can be seen from Figure 2(D) in the main manuscript: (i) If the new gap $l^{'} \geq k$, the remaining gap $l - (l^{'} + k)$ is not big enough to accommodate a second nucleosome to its right, as l has maximum value $3k - 1$ within our approximation. But, a second nucleosome can indeed bind in the space $l^{'}$ with an average timescale of $T_{l^{'}}$. (ii) If the new gap $l^{'} < k$, a second nucleosome can only bind if the gap $l - (l^{'} + k) \geq k$. Assuming that is the case, the first binding is followed by either its immediate dissociation (with further delay of $\frac{k_{\rm off}}{\widetilde{X}_{l,l'}} T_l$), or dissociation of nucleosome I (with further delay of $\frac{k_{\rm off}}{\widetilde{X}_{l,l'}} T_{l'}$), or binding of a second nucleosome in $l - l^{'} - 2k + 1$ positions (with further delay of $\frac{1}{2k_{\rm off}} + \frac{1}{2} T_{l'+k+\delta} + \frac{1}{2} T_{l'}$, as in case 3), where δ is the space between the first and the second nucleosome. (iii) Finally for $l^{'} < k$ and $l - (l^{'} + k) < k$, there is not enough space for second binding. Hence the subsequent delay is $1/2k_{\rm off} + T_l/2 + T_{l^{'}}/2$ just as in case 3 – this is equivalent to setting $\tilde{k}_{\rm on} = 0$ in Eq. **5** and in the expression for $\widetilde{X}_{l,l'}$.

4 Modified equations to include the effect of DNA sequence and remodelers

As discussed in the main manuscript, the effect of spatial heterogeneity in histone-DNA interaction is captured through spatially varying off rates. The dissociation rates get contribution from the local potentials V_i (which captures effect of DNA sequence and basal remodeling) where i refers to the i^{th} bp – see Eq. **1** of main text. Below we write the explicit equation for T_l, which are modification of Eqs. **3-6** in main manuscript, replacing uniform $k_{\rm off}$ by specific local $k_{\rm off}^{(i)}$ where, i is the left most bp of the nucleosome positioned between $[i, i + k - 1]$. We have used two types of situations in the main manuscript – the target patch is to the right or left of the barrier:

(A). Target patch to the right of the barrier: For example, when the barrier is at TSS and m-patch is in the coding region (see Figure 4(A) of the main manuscript). In this situation, the equations can be written as:

Case 1: For $l_{\rm min} \leq l < k$:

$$T_l \; - \sum_{\tilde{l}=l+k}^{3k-1} P(\tilde{l})\, T_{\tilde{l}} \; = \; \frac{1}{k_{\rm off}^{(l+1)}} \tag{S6}$$

Case 2: For $k \leq l < (l_1 + m + k)$:

$$T_l \; - \; \frac{k_{\rm off}^{(l+1)}}{\lambda_l} \sum_{\tilde{l}=l+k}^{3k-1} P(\tilde{l})\, T_{\tilde{l}} \; = \; \frac{1}{\lambda_l} \tag{S7}$$

where, $\lambda_l = k_{\rm off}^{(l+1)} + k_{\rm on}(l - k + 1)$.

Case 3: For $(l_1 + m + k) \leq l < 2k$:

$$T_l \; - \; \frac{k_{\rm on}}{\lambda_l} \sum_{l'=m+l_1}^{l-k} \Big[\frac{1}{k_{\rm off}^{(l+1)} + k_{\rm off}^{(l'+1)}} + \frac{k_{\rm off}^{(l'+1)}}{k_{\rm off}^{(l+1)} + k_{\rm off}^{(l'+1)}} T_l + \frac{k_{\rm off}^{(l+1)}}{k_{\rm off}^{(l+1)} + k_{\rm off}^{(l'+1)}} T_{l'} \Big] - \frac{k_{\rm off}^{(l+1)}}{\lambda_l} \sum_{\tilde{l}=l+k}^{3k-1} P(\tilde{l})\, T_{\tilde{l}} \; = \frac{1}{\lambda_l} \tag{S8}$$

Case 4: For $2k \leq l < 3k$:

$$T_l \; - \; \frac{k_{\rm on}}{\lambda_l} \sum_{l'=m+l_1}^{k-1} \Big[\; \frac{1}{X_{l,l'}} \; + \; \frac{k_{\rm off}^{(l'+1)}}{X_{l,l'}} T_l \; + \; \frac{k_{\rm off}^{(l+1)}}{X_{l,l'}} T_{l'} \; + \; \frac{\tilde{k}_{\rm on}}{X_{l,l'}} \sum_{\delta=0}^{l-l'-2k} \Big\{ \frac{1}{k_{\rm off}^{(l'+1)} + k_{\rm off}^{(l'+k+\delta+1)}} \; +$$

$$\frac{k_{\rm off}^{(l'+1)})}{k_{\rm off}^{(l'+1)}+k_{\rm off}^{(l'+k+\delta+1)}}T_{l'+k+\delta} \;+\; \frac{k_{\rm off}^{(l'+k+\delta+1)}}{k_{\rm off}^{(l'+1)}+k_{\rm off}^{(l'+k+\delta+1)}}T_{l'}\Big\}\Big] \;-\; \frac{k_{\rm on}}{\lambda_l}\sum_{l'=k}^{l-k}P(l')\,T_{l'} \;=\; \frac{1}{\lambda_l} \tag{S9}$$

For Eq. S9, $X_{l,l'} = k_{\rm off}^{(l+1)} + k_{\rm off}^{(\tilde{l}+1)} + \tilde{k}_{\rm on}(l-l'-2k+1)$ and

$$\tilde{k}_{\rm on} = \begin{cases} 0 & \text{if } \hat{\ell} < 0 \\ k_{\rm on} & \text{if } \hat{\ell} \geq 0 \end{cases}$$

where, $\hat{\ell} = l - l' - 2k + 1$.

Note that the left most bps of the nucleosomes undergoing dissociation are at locations $(l+1)$, $(l'+1)$, and $(l'+k+\delta+1)$, in different cases in the above equations.

(B). The target patch to the left of the barrier:

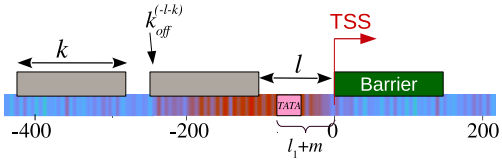

Figure S4: Schematic figure showing the situation where the m patch is to the left of the barrier.

For example, when barrier is at TSS and TATA box is the target patch (see Figure S4). In this condition, the above equations will be slightly modified as follows: Since we measure l from the barrier head, the distances to the left will be in negative. Therefore, in Eqs. S6 and S7 above, $k_{\rm off}^{(l+1)} \rightarrow k_{\rm off}^{(-l-k)}$. Similarly, in Eqs. S8 and S9 above, $k_{\rm off}^{(l'+1)} \rightarrow k_{\rm off}^{(-l'-k)}$ and $k_{\rm off}^{(l'+k+\delta+1)} \rightarrow k_{\rm off}^{-(l'+k+\delta)-k}$ other things remain same. Note that the left most bps of the nucleosomes undergoing dissociation are now at locations $(-l-k)$ (see Figure S4), $(-l'-k)$, and $-(l'+k+\delta)-k$, in different cases in the above equations.

5 Partially stable barrier

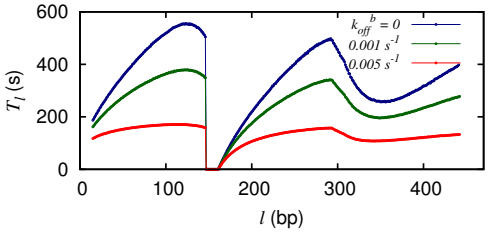

Figure S5: Effect of short lived barrier. Blue curve: the barrier is highly stable with its dissociation rate equal to zero. Note, the nucleosome binding and dissociation rates are $12s^{-1}$ and $0.01s^{-1}$ respectively. Green and Red curves: barrier is short lived with dissociation rates $0.001s^{-1}$ (10 times more stable than nucleosomes) and $0.005s^{-1}$ (5 times more stable than nucleosomes) respectively. The rebinding rate of the barrier for both green and red are $12s^{-1}$. The average exposure times for data in the green and the red curves are $T_{\rm av} = 211$s and $T_{\rm av} = 134$s respectively as compared to $T_{\rm av} = 259$s corresponding to the blue curve.

In our model, we have considered the barrier as highly stable. However, in reality, such barriers would have a long but finite life time and wouldn't be infinitely stable. Therefore, it is a fair question to ask

how our results would get affected if we relax this assumption of infinite stability. In this section, we performed simulations incorporating the kinetics of the barrier along with the nucleosomes such that, the barrier can also disassemble and reassemble with a given rate. We assumed barrier disassembly rate 5 or 10 times slower than the nucleosome disassembly rate ($0.01s^{-1}$). The results are shown in Figure S5. We find that on making the barrier partially unstable, the exposure times are reduced but still are comparable (see the figure caption). Moreover, the BL shape of the curve is preserved. When the barrier is allowed to disassemble, it offers more possibilities of patch coverage leading to reduction in average timescales.

6 Changing nucleosome size: mimicking wrapping/unwrapping at nucleosome edges

Thermal wrapping/unwrapping has a timescale of the order of milliseconds [2] but the typical timescale of some TFs and TBP binding is of the order of seconds to minutes [3]. Since our aim is to figure out timescales relevant for TBP-like proteins binding, the unwrapping/wrapping at the nucleosome entry/exit may not be relevant for this problem. However, we can indirectly investigate the fluctuation in base-pair contact of the nucleosomes by varying the size of the nucleosomes, k. Data for different k values (ranging from 120 to 147 bp) is shown in Figure S6.

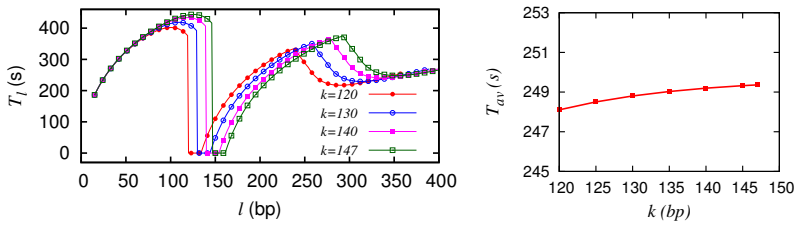

Figure S6: Left: Results of T_l versus l for different k. Right: $T_{\rm av}$ calculated for different k. We find that on varying k, whereas T_l are different at different l, $T_{\rm av}$ has almost no change.

From Figure S6(left), we note that at specific locations (namely l close to k or $k+m$), suddenly the time T_l may drop from high to low value (or vice versa) due to variation in k, i.e., local exposures times may suffer variations depending on initial nucleosome arrangements, as a result of change in nucleosome size. Yet, for generic nucleosome arrangements, i.e. for l-averaged mean exposure time $T_{\rm av}$ shown in right figure there is only a small variation ($\sim$ 2s) over the k range considered. We may interpret this in another way – if there is wrapping/unwrapping happening on a fast timescale (say over $\sim$ms), the averaged exposure time ($T_{\rm av}$) estimated over longer observation times of concern in this paper ($\sim$s) would hardly get affected (think of the numbers in Figure S6(right)) by such events, although there may be occasional fluctuations in the observed exposure times.

7 Timescales of patch coverage in the coding region

Similar to the Figure 4(B) for gene *YIL018W* shown in the main manuscript, in Figure S7, we show the T_l versus l curves for gene *YCR012W*. All other parameters are the same. The BL shape of the simulation (blue) and theory (red) curves can be again noted, which are quite different from the local $1/k_{\rm off}^{(i)}$s (gray curve). Using Eq. **2** in the main manuscript, we get $T_{\rm av}$ = 1590s (theory) and 1720s (simulation). These values are much higher than those obtained for gene *YIL018W*, $T_{\rm av}$ = 122s (theory) and 136s (simulation), indicating comparatively slower nucleosomal activity in the +1 nucleosome region of the gene *YCR012W*. Green curve in Figure S7 shows that nucleosome destabilising remodeling leads to lowering of timescales.

8 Effect of changing $\langle V_i \rangle$ and $k_{\rm on}$ on exposure times

Depending upon the nucleosome density and remodeling activities in different organisms/cell types, local potential V_i and its average $\langle V_i \rangle$ may vary. Effect of the local variation in potential on T_l and $T_{\rm av}$ has

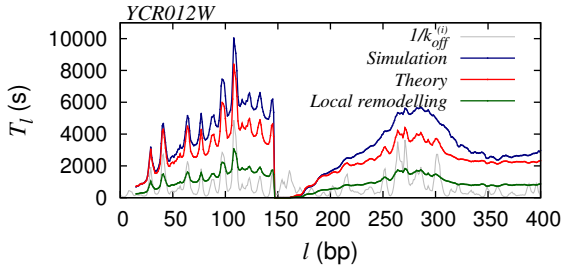

Figure S 7: T_l versus l for gene *YCR012W*, simulations (blue), theory (red), $1/k_{\rm off}^{(i)}$ (gray) and, theory with local remodeling that makes the +1 nucleosome less stable (green). Parameters are $k = 147$, $l_1 = 5$, $m = 10$, $k_{\rm on} = 12.0s^{-1}$, $U_i = 1k_{\rm B}T$.

been shown in Figures 4 and 5 of the main manuscript. In Figure S8(A) and (B), we show the change of exposure times on changing $\langle V_i \rangle$. The range of $T_{\rm av}$ seen here is similar to that found across the genome as shown in Figure 7 (main manuscript).

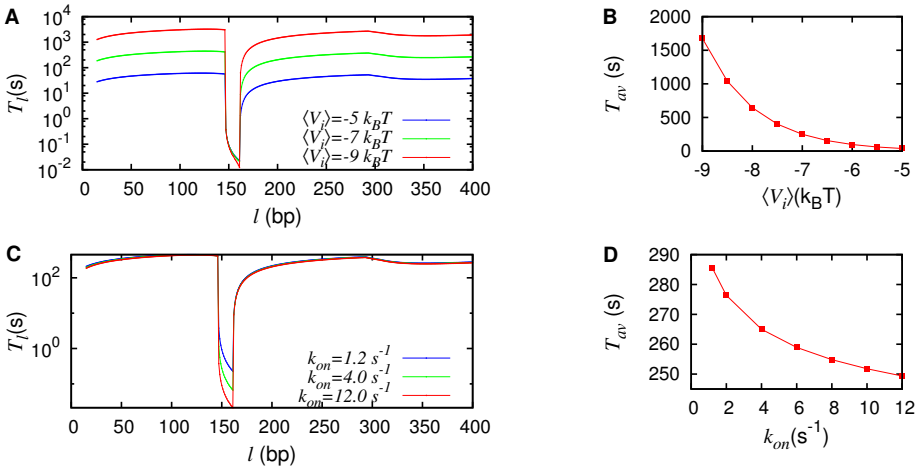

Figure S 8: (A) T_l versus l plot for different $\langle V_i \rangle$. (B) $T_{\rm av}$ corresponding to different $\langle V_i \rangle$. For (A) and (B) nucleosome binding rate is taken to be $12s^{-1}$. (C) T_l versus l plot for different $k_{\rm on}$. (D) $T_{\rm av}$ as a function of $k_{\rm on}$. For (C) and (D) $\langle V_i \rangle = -7k_BT$. All the data shown here are for a uniform sequence.

Furthermore, in this manuscript, we have assumed that the sequence dependence of histone-DNA interaction only comes through the dissociation rate $k_{\rm off}^i$ (see Eq. 1 of main manuscript) and the binding rate of nucleosomes $k_{\rm on}$ is sequence independent. However, as seen for TFs, nucleosomes may also have different binding rates; here we test how the exposure timescales would alter if we vary k_{on}. As we see from Figures S8 (C) and (D) the changes are minimal for variation of $k_{\rm on}$ by a factor of 10.

9 Explanation of the peculiarity seen in $T_{\rm av}$ Vs l_1 curve for GAL1 gene

In Figure 4(F) of the main manuscript, contrary to intuition, we find that $T_{\rm av}$ increases with increasing l_1. Here we provide a mechanistic explanation for this behavior.

As explained in the main manuscript, the barrier is present at site 1 and we calculate the $T_{\rm av}$ for patches 2, 3 and 4 for which l_1 increase from 2 bp to 84 bp. In the coverage of these Gal4 binding sites, the two events that dominate are the following: The dissociation of the nucleosome next to the Gal4 site (2, 3 or 4), followed by the binding of a nucleosome that covers the site. When there is no sequence effect, the rate of the first dissociation do not vary with l_1, while the rate of the next binding increases with l_1 as the number of binding possibilities increase with l_1. This leads to $T_{\rm av}$ decreasing as l_1 increase as shown in red curve in Figure 4(F) of main manuscript. But in the presence of sequence effects, the

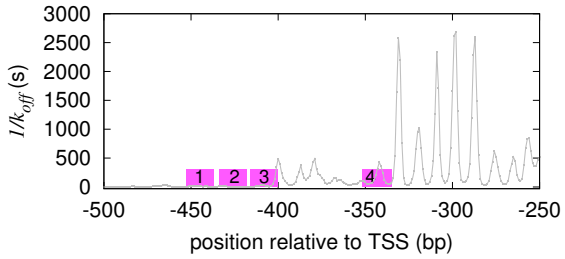

Figure S9: Gal4 binding sites plotted with the sequence dependent dissociation timescales aided with remodeling effects. For Figure 4(F) of main manuscript, the barrier (due to Gal4 binding) is at site 1 and we calculate the first passage exposure times of patches 2, 3, and 4. The timescales adjacent to patch 4 is very high ($\sim$ 2000 s) that causes slow dissociation of the bounding nucleosome hence higher $T_{\rm av}$.

dissociation rate vary with spatial location as seen in Figure S9 below. Note that in this figure, next to the site 4, the dissociation timescales are high (rates are low) while next to sites 2 or 3, the dissociation timescales are relatively lower. So, the first unbinding itself will get much more delayed when the m patch is at site 4 as opposed to 2 or 3. This dissociation-induced delays supersede the increase in binding probabilities due to variation in l_1.

10 Effect of sliding kinetics on exposure times

Here we introduce sliding as another kinetic event along with binding and dissociation of nucleosomes. Since the sliding mechanism of yeast nucleosomes is not well known, we used the sliding rule of Florescu et. al. [4] where they model experimentally observed sliding of nucleosomes by human chromatin remodelers *ISWI/ACF* [5, 6, 7]. The rules for sliding are as follows: We slide a nucleosome either to its left or to its right if there is a gap $>$ 15bp besides it. Rate of sliding is taken to be $k_s = 0.0017$ s^{-1} [6, 4] and the sliding step is 10bp. In Figure S10, we plot the simulation results for the gene $YCR012W$.

In Figure S10(A) we are comparing the same data given in Figure S7 (blue curve, without local remodeling-assisted dissociation, i.e. $U_i = 0$) with the new result in the presence of sliding (pink curve). We see that sliding-moves lower the timescales T_l, yet maintain the overall BL shape of the curve. For comparison, the estimated T_l from our theory is also shown (red curve).

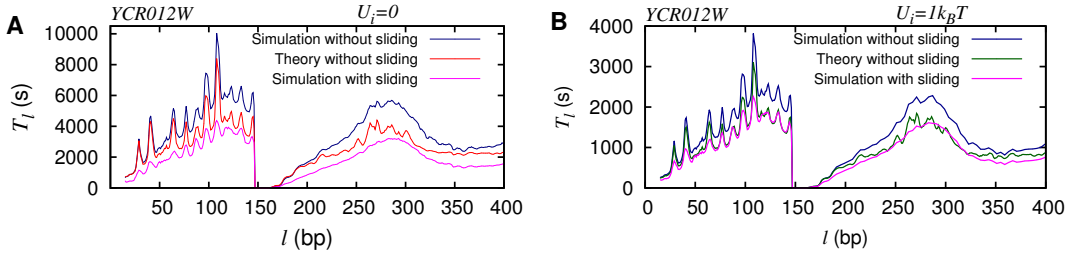

Figure S10: Effect of sliding on T_l Vs l curves for gene $YCR012W$: (A) without local remodeling-assisted dissociation, $T_{\rm av}$ = 1722s and 880s corresponding to the blue (without sliding) and pink (with sliding) curves, respectively. Curve from our theory (without sliding) is shown in red. (B) with local remodeling-assisted dissociation, $T_{\rm av}$ = 640s and 447s corresponding to the blue (without sliding) and pink (with sliding) curves, respectively. Curve from our theory (with local remodeling-assisted dissociation, and without sliding) is shown in green.

We have seen that both sliding and local remodeling-assisted dissociation ($U_i > 0$) reduce the timescales T_l. Given that local remodeling-assisted dissociation is present in locations like +1 regions and promoters, it would be interesting to know the joint effect of both these factors. In Figure S10(B), we compare the results for T_l, with local remodeling-assisted dissociation ($U_i > 0$), in the absence (blue curve) and presence (pink curve) of nucleosome sliding-moves. Note that the separation of the pink and blue curves in Figure S10(A) is more in comparison to the ones in Figure S10(B). Thus in the presence

of local remodeling-assisted dissociation, additional sliding-moves have lesser effect on the timescales. Since the local remodeling-assisted dissociation moves happen much faster than sliding-moves the latter is less relevant. For comparison we also show our theory curve (green, with local remodeling-assisted dissociation).

References

[1] Krapivsky PL, Ben-Naim E (1994) Collective properties of adsorption-desorption processes. *J Chem Phys* 100:6778–6782.

[2] Li G, Levitus M, Bustamante C, Widom J (2005) Rapid spontaneous accessibility of nucleosomal DNA. *Nat. Struct. Mol. Biol.* 12:46–53.

[3] Perez-Howard GM, Weil PA, Beechem JM (1995) Yeast TATA Binding Protein Interaction with DNA: Fluorescence Determination of Oligomeric State, Equilibrium Binding, On-Rate, and Dissociation Kinetics. *Biochemistry* 34:8005–8017.

[4] Florescu AM, Schiessel H, Blossey R (2012) Kinetic Control of Nucleosome Displacement by ISWI/ACF Chromatin Remodelers. *Phys Rev Lett* 109:1–5.

[5] Yang JG, Madrid TS, Sevastopoulos E, Narlikar GJ (2006) The chromatin-remodeling enzyme ACF is an ATP-dependent DNA length sensor that regulates nucleosome spacing. *Nat Struct Mol Biol* 13:1078–1083.

[6] Racki LR, et al. (2009) The chromatin remodeller ACF acts as a dimeric motor to space nucleosomes. *Nature* 462:1016–1021.

[7] Blosser TR, Yang JG, Stone MD, Narlikar GJ, Zhuang X (2009) Dynamics of nucleosome remodelling by individual ACF complexes. *Nature* 462:1022–1027.